Renewable Energy 131 (2019) 730–736

Contents lists available at ScienceDirect

Renewable Energy

journal homepage: www.elsevier.com/locate/renene

Colour properties and glazing factors evaluation of multicrystalline based semi-transparent Photovoltaic-vacuum glazing for BIPV application

Aritra Ghosh*, Senthilarasu Sundaram, Tapas K. Mallick

Environmental and Sustainability Institute, University of Exeter, Penryn, Cornwall, UK

ARTICLE INFO

Article history:
Received 2 May 2018
Received in revised form
4 July 2018
Accepted 18 July 2018
Available online 20 July 2018

Keywords:
Adaptive
Glazing
SF/SHGC
PV
Vacuum
Transmission
BIPV
Building

ABSTRACT

Low heat loss vacuum glazing offers high heat insulation for indoor space, which reduces the building's heating energy demand. However, the transparent nature of this glazing allows similar daylight to double glazing that creates discomfort glare. Double pane semi-transparent type photovoltaic (PV) glazing introduces control of solar heat gain, daylight and generates clean electricity. The transparent portion between regularly distributed PV cells allows light penetration. Addition of these two technologies can offer low heat loss PV-vacuum glazing that will control heat loss, heat gain, and daylight and generate renewable power. In this work, two different areas of multicrystalline PV cells were employed to form 35% and 42% transparent PV-vacuum glazing. Spectral characterisation, glazing factor and entering light quality through the transparent part of this PV-vacuum glazing were evaluated. Colour rendering and correlated colour temperature of this glazing were compared with an electrically actuated switchable suspended particle device glazing.

1. Introduction

In developed countries, commercial and residential buildings account 20–40% of total consumed energy [1]. Indoor space heating, cooling and artificial lightings are the responsible sectors for this high consumption. Use of small window area can reduce energy consumption by reducing heating and cooling load. However, this small size window opening restricts the penetration of natural daylight into the indoor space which is essential for occupant's health, mood and biological benefits [2]. Building windows maintain the external viewing from indoor while ensuing heat loss and heat gain both.

Ordinary single or double glazing is not energy efficient as it allows high heat loss, heat gain and also allows direct daylight which generates glare [3]. Buildings in cold climate, particularly in northern latitude countries, increase the energy demand for space heating due to high heat losses through poorly insulated glazing [1]. Evacuated (Vacuum) glazing is the potential device for this location. In a vacuum glazing, vacuum (<0.1Pa) is maintained between two glass panes as shown in Fig. 1. To withstand outside atmospheric pressure metal based support pillars are provided between two glass panes. These pillars have negligible visual obstructions [4]. Presence of vacuum reduces conductive and convective heat flow. To reduce radiative heat transfer one of the glass pane is coated with low emissivity (low-e) coating [5]. First vacuum glazing was manufactured at the University of Sydney [6,7] using high temperature solder edge sealing, which degrades the low-e coating. Low temperature indium alloy edge sealing based vacuum glazing was fabricated at the University of Ulster [8] to enable the durability of low-e coating. Presently at Loughborough University Cerasolzer type CS186 was used for low temperature edge sealing [9]. Transparent support pillars are also now investigated by Ref. [10]. Using indoor characterisation [11] and finite element simulation [12] showed that vacuum glazing offers very low overall heat transfer coefficient. Low overall heat transfer was also found from outdoor characterisation at temperate climate location (Dublin) [4,13].

However, due to higher transparency, vacuum glazing offers similar daylight penetration to double glazing which creates

* Corresponding author.
E-mail addresses: a.ghosh@exeter.ac.uk (A. Ghosh), t.k.mallick@exeter.ac.uk (T.K. Mallick).

https://doi.org/10.1016/j.renene.2018.07.088

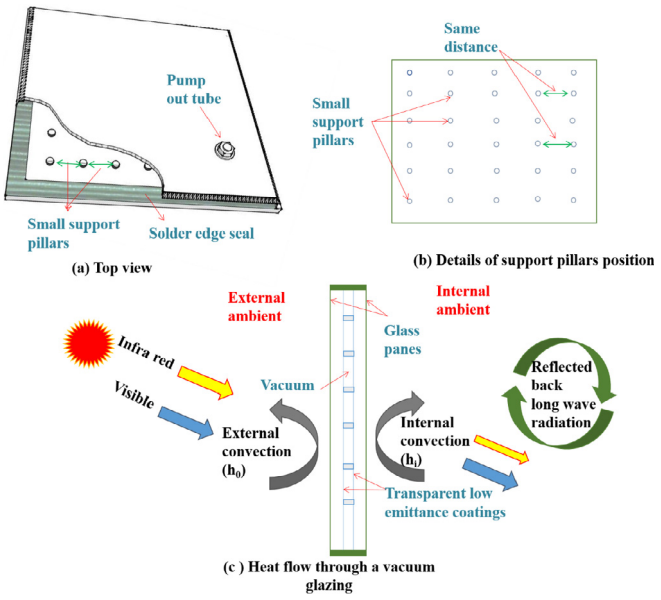

Fig. 1. Details of vacuum (evacuated) glazing.

discomfort glare [4]. Control over this higher daylight penetration is essential. Presently solar gain and excessive daylight control glazings include switchable transparent electrochromic (EC) [14], suspended particle device (SPD) [15–20], liquid crystal (LC) [21] [22] and static transparent photovoltaic [23]. Addition of switchable glazing material with vacuum glazing can reduce daylight penetration. Switchable SPD [16,24] and EC [25,26] glazing attached with vacuum glazing showed the feasibility of this combined technologies. However, this switchable glazing needs power requirement to switch from one state to another. For large-scale façade application, this power requirement can enhance the building's switching energy demand.

Photovoltaic (PV) based glazing is suitable for limiting solar heat gain and daylight whereas it generates clean electricity. PV glazing consists of two glass panes where PV materials are sandwiched between them. PV glazing elements [23] replace the buildings traditional glazing elements and work as buildings skin which is referred to building integrated photovoltaic (BIPV) [27]. In a PV glazing, PV device includes silicon solar cell, cadmium telluride (CdTe) [28], amorphous silicon (a-Si) [29], copper indium selenide/sulfide (CIGS), DSSC [30,31] and perovskite [32] type. However, perovskite and DSSC based PV needs stability under moisture and ambient condition before being considered for practical PV glazing application [33,34]. Among the 2nd generation CdTe, CIGS and a-Si, a-Si has been investigated extensively for glazing application as see through a-Si allows natural daylight [35]. Traditional crystalline solar cell for PV glazing is superior due to its mature, low cost [36–38] and highly durable technology. However, PV glazing covered by opaque silicon PV stops viewing from indoor space to outdoor and restricts daylight penetration into indoor space. For building façade and glazing application, semitransparency is essential. Silicon PV based semi-transparent PV glazing remains regularly distributed opaque PV cells, which offer transparent gaps between the PV cells as shown in Fig. 2. In this type of glazing, incident solar radiation on the portion covered by opaque PV cell generates clean electricity and remaining part is absorbed by PV material. Transparent portion allows incident solar radiation, which allows solar heat gain, daylighting and viewing through the glazing [39]. From a theoretical analysis of semi-transparent type

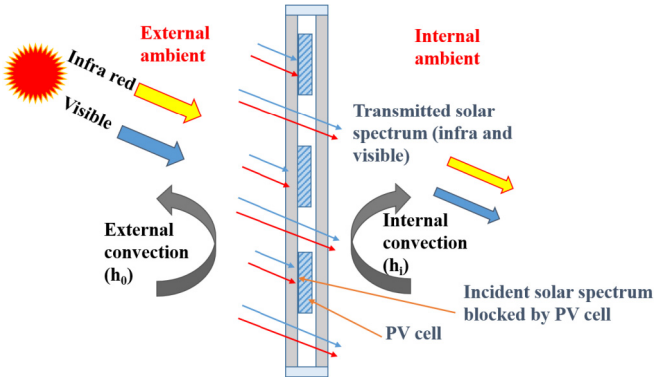

Fig. 2. Schematic of silicon solar cell based semi-transparent type PV glazing.

PV glazing, it was found that glazing area covered by higher percentage of solar cell allows lower heat gain [40].

Addition of PV and vacuum glazing, which is low heat loss power generating glazing (combined PV-Vacuum glazing), can be the best solution as it can contract energy demand, admit comfortable daylight as well as generate clean electricity. A combined PV-vacuum glazing was reported where PV was 20% transparent a-Si type. This laminated combined glazing was fabricated using four glass panes while average glazing transmittance was 0.08 [41].

In this paper, first time multicrystalline based combined semi-transparent PV-vacuum glazing has been introduced for low energy adaptive retrofit or new building. In the combined system, the total number of glass panes were three as shown in Fig. 3. The transmittance of this glazing was achieved from non-covered area by PV. Two different area of PV cells were employed in this investigation. In this PV –vacuum combined glazing, overall glazing transmittances due to the presence of PV were 35% (for the first case) and 42% for the second case.

Comfortable daylight offers a higher performance of work. To ensure buildings occupants physical, mental wellbeing and visual comfort not only quantity but the quality of light is also essential [42,43]. Quality of light is assessed by colour rendering index (CRI) and correlated colour temperature (CCT) [44]. When glazing filters the daylight, spectral variation of glazing material influence the colour rendering. Entering solar spectrum also has an influence on the building materials durability which can be accessed by solar skin protection factor (SSPF) and solar material protection factor (SMPF) [45,46]. As PV-vacuum glazing is considered to be a future

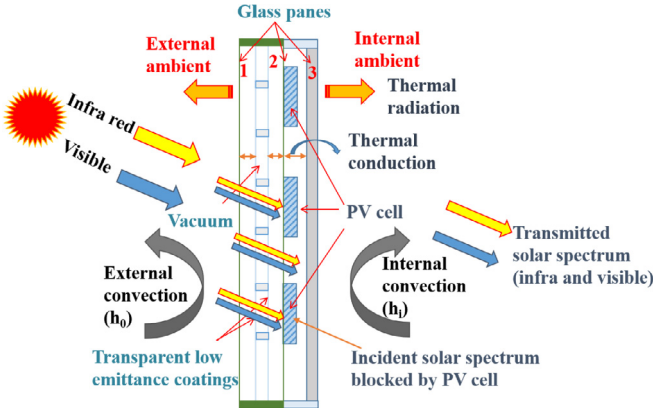

Fig. 3. Schematic of three glass panes semi-transparent PV –Vacuum glazing.

fenestration technology, its CCT, CRI and glazing factors need to be evaluated.

Optical properties, glazing factors, CCT, CRI are evaluated for this combined glazing and compared with a single and a vacuum glazing. This 35% and 42% transparent combined glazing's colour rendering property has also been compared with 30% and 40% transparent switchable SPD glazing.

2. Methodology

2.1. Optical properties

Optical properties of combined PV-vacuum glazing was achieved from calculated transmittance and reflectance values in ultraviolet, luminous and solar region. $S_{uv}(\lambda)$ is relative spectral distribution of ultraviolet solar radiation. D_{65} is the relative spectral distribution of the illuminant D65, V(λ), $V(\lambda)$ is the spectral luminous efficiency of a standard photopic observer, $S(\lambda)$ relative spectral distribution of solar radiation and $\Delta\lambda$ is the wavelength interval. $T(\lambda,\alpha)$ and $R(\lambda,\alpha)$ are the spectral transmission and reflection of glazing. The angle of incidence is α and for normal incidence it is 0 [47].

$$\text{UV transmittance } \tau_{uv}(\alpha) = \frac{\sum_{\lambda=280nm}^{380nm} S_{uv}(\lambda)T(\lambda,\alpha)\Delta\lambda}{\sum_{\lambda=380nm}^{380nm} S_{uv}(\lambda)\Delta\lambda} \quad (1)$$

$$\text{Luminous transmission } \tau_v(\alpha) = \frac{\sum_{\lambda=380nm}^{780nm} D_{65}(\lambda)T(\lambda,\alpha)V(\lambda)\Delta\lambda}{\sum_{\lambda=380nm}^{780nm} D_{65}(\lambda)V(\lambda)\Delta\lambda} \quad (2)$$

$$\text{Luminous reflection } \rho_v(\alpha) = \frac{\sum_{\lambda=380nm}^{780nm} D_{65}(\lambda)R(\lambda,\alpha)V(\lambda)\Delta\lambda}{\sum_{\lambda=380nm}^{780nm} D_{65}(\lambda)V(\lambda)\Delta\lambda} \quad (3)$$

$$\text{Solar transmission } \tau_s(\alpha) = \frac{\sum_{\lambda=300nm}^{2500nm} S(\lambda)T(\lambda,\alpha)\Delta\lambda}{\sum_{\lambda=300nm}^{2500nm} S(\lambda)\Delta\lambda} \quad (4)$$

$$\text{Solar reflection } \rho_s(\alpha) = \frac{\sum_{\lambda=300nm}^{2500nm} S(\lambda)R(\lambda,\alpha)\Delta\lambda}{\sum_{\lambda=300nm}^{2500nm} S(\lambda)\Delta\lambda} \quad (5)$$

$$\text{Solar/visible absorption} a_{(s/v)}(\alpha) = 1 - \tau_{(s/v)}(\alpha) - \rho_{(s/v)}(\alpha) \quad (6)$$

2.2. Glazing factors

Transmitted solar energy through a glazing is indicated by solar factor (SF) [46].

$$g = \tau_s + q_i = \tau_s + \frac{\frac{A_{s1}+A_{s2}+A_{s3}}{h_e} + \frac{A_{s2}+A_{s3}}{d_{1,2}} + \frac{A_{s3}}{d_{2,3}}}{1/h_i + 1/h_e + 1/d_{1,2} + 1/d_{2,3}} \quad (7)$$

where A_{s1}, A_{s2}, A_{s3} are the solar absorbance of the first, second and third glass panes, $d_{1,2}$ and $d_{2,3}$ are the thermal conductance between the first and second glass panes and second and third glass panes respectively, h_e and h_i are the external and internal heat transfer coefficient, τ_s is solar transmittance.

Presence of ultraviolet (UV) into the entering solar radiation in a building is responsible for degradation of building materials, discolouration of wall painting, books, wooden materials, furniture. Silica made glass materials are capable to block UV, still significant amount of UV penetrates through the glazing into indoor space. Solar material protection factor (SMPF) and solar skin protection factor (SSPF) determine how well a glazing or glazed façade can protect material of a building and the skin damage of building occupant from UV. SMPF and SSPF are the integrated values of solar spectrum from 300 nm to 600 nm and 300 nm–400 nm respectively. SMPF and SSPF range between 0 and 1, where zero indicates the protection level is low and one indicates the protection level is high [45,46].

Solar material protection factor (SMPF)

$$SMPF = 1 - \frac{\sum_{\lambda=300nm}^{600nm} T(\lambda)C_\lambda S_\lambda \Delta\lambda}{\sum_{\lambda=300nm}^{600nm} C_\lambda S_\lambda \Delta\lambda} \quad (8)$$

where $C_\lambda = e^{-0.012\lambda}$

And solar skin protection factor (SSPF)

$$SSPF = 1 - \frac{\sum_{\lambda=300nm}^{400nm} T(\lambda)E_\lambda S_\lambda \Delta\lambda}{\sum_{\lambda=300nm}^{400nm} E_\lambda S_\lambda \Delta\lambda} \quad (9)$$

E_λ CIE erythermal effectiveness spectrum.

2.3. CCT and CRI

Quality and quantity of entering daylight are characterised by correlated colour temperature (CCT) and colour rendering index (CRI). Perfect transmitted daylight should have CCT from 3000 K to 7500 K while CRI close to 100 is required. CRI below 90 is not suitable for glazing application.

CCT was calculated from McCamy's Eq. (10) [48].

$$CCT = 449n^3 + 3525n^2 + 6823.3n + 5520.33 \quad (10)$$

where

$$n = \frac{(x - 0.3320)}{(0.1858 - y)}$$

$$x = \frac{X}{X+Y+Z} \quad y = \frac{Y}{X+Y+Z}$$

$$X = \sum_{380nm}^{780nm} D_{65}(\lambda)\tau(\lambda)\overline{x}(\lambda)\Delta\lambda \quad (11)$$

$$Y = \sum_{380nm}^{780nm} D_{65}(\lambda)\tau(\lambda)\overline{y}(\lambda)\Delta\lambda \tag{12}$$

$$Z = \sum_{380nm}^{780nm} D_{65}(\lambda)\,\tau(\lambda)\overline{z}(\lambda)\Delta\lambda \tag{13}$$

X, Y and Z are the tristimulus values which represent the three-colour perception values of the human eye response, Luminous transmittance values τ_v, D65(λ) is the spectral power distribution of CIE standard illuminant D65, V(λ) is the photopic luminous efficiency function of the human eye and $\Delta\lambda = 10$ nm.

CRI is given by

$$CRI = \frac{1}{8}\sum_{i=1}^{8}\left[100 - 4.6\left\{\sqrt{\left(U^*_{t,i}-U^*_{r,i}\right)^2+\left(V^*_{t,i}-V^*_{r,i}\right)^2+\left(W^*_{t,i}-W^*_{r,i}\right)^2}\right\}\right] \tag{14}$$

Conversion into the CIE 1964 uniform colour space system for each test colours the conversion is performed using colour space system $W^*_{t,i}$, $U^*_{t,i}$, $V^*_{t,i}$ whereas $W^*_{r,i}$, $U^*_{r,i}$, $V^*_{r,i}$ represents for each test colours, lighted by the standard illuminant D65 without the glazing

$$W^*_{t,i} = 25\left(\frac{100Y_{t,i}}{Y_t}\right)^{1/3} - 17 \tag{15}$$

$$U^*_{t,i} = 13W^*_{t,i}\left(u'_{t,i} - 0.1978\right) \tag{16}$$

$$V^*_{t,i} = 13W^*_{t,i}\left(V'_{t,i} - 0.3122\right) \tag{17}$$

3. System integration & experiment

One vacuum glazing from NSG Spacia and one single glazing from Pilkington dimensions of 0.2 m × 0.35 m were employed to fabricate combined glazing as shown in Fig. 4. One 0.155 m × 0.155 m multicrystalline solar cell was placed on the top of this vacuum glazing. This one offered 42% overall transparency of combined PV-vacuum glazing. For another glazing, two 0.125 m × 0.125 m multicrystalline PV cells were connected in series, placed on the vacuum glazing. This system offered 35% overall transmission. Sylgard 184 encapsulation was poured on top of the PV. Single glazing was placed on the encapsulated PV. Edge of this combined glazing was sealed by transparent silicon. Transparency of this type semi-transparent glazing can vary during fabrication process using different size of solar cell. Optical characterisation of this glazing was performed using one UV-VIS-NIR spectrophotometer.

4. Results

4.1. Spectral performance

Transmission for this type of semi-transparent PV-vacuum glazing showed two different regions: covered by PV cells and non-covered by PV cells or transparent portion between PV cells. Transmission of the PV cells occupied regions are negligible due to the opaque nature of this PV cells. Fig. 5 shows the UV, visible and NIR transmittance and reflectance of the transparent part of the PV-vacuum glazing. For comparison single glazing, vacuum glazing transmissions are also shown, as they were an integral part of the combined glazing. UV, visible and solar transmittance were calculated using Eqs. (1), (2) and (4) respectively. Only normal incident transmittance was measured for this work. For this combined glazing, UV, luminous and solar transmittances were 18%, 64% and 33% respectively. Lower solar transmittance was achieved due to the presence of low-e coating in the vacuum glazing. Table 1 illustrates all transmissions and reflections of the three glazing systems. Combined glazing has more influence from vacuum

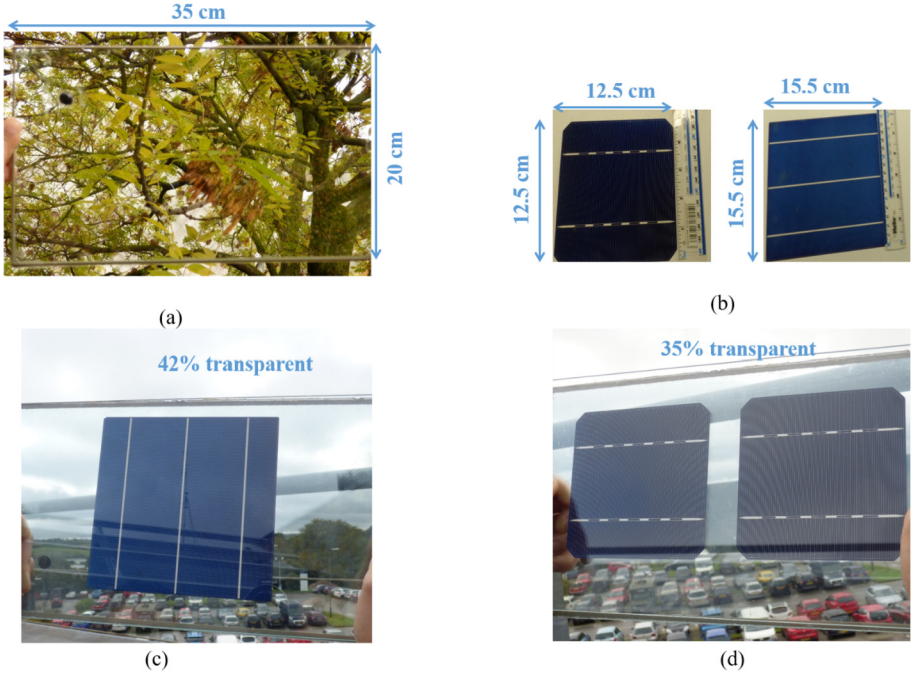

Fig. 4. (a) Viewing through vacuum glazing, (b) two different dimensions PV cells, (c) 42% transparent PV-vacuum glazing (d) 35% PV-vacuum glazing.

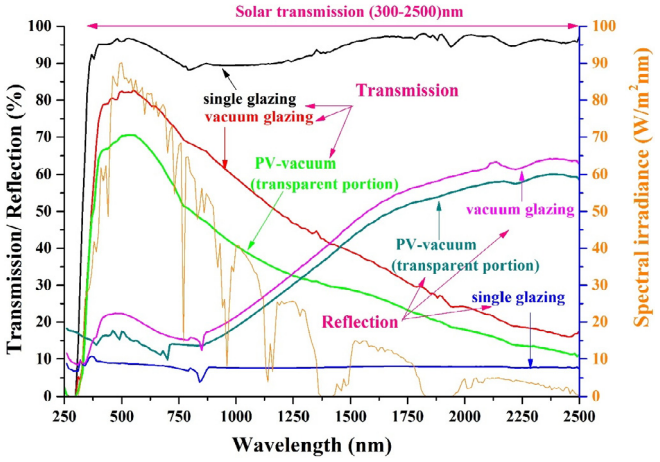

Fig. 5. Transmission and reflection of non-PV covered part of combined PV-Vacuum glazing, single, vacuum glazing (280 nm-2500 nm).

Table 3
CRI and CCT for different glazings.

	CRI	CCT
35% and 42% combined PV-Vacuum glazing	96.7	6360 K
Single glazing	98.7	6545 K
Vacuum glazing	97.7	6532 K
30% transparent SPD	87	4900 K
40% transparent SPD	91	5202 K

and wood become discolours behind glass inside buildings easily whereas human beings do not get sunburnt or tanned inside a building.

4.3. CCT and CRI

Correlated colour temperature (CCT) and colour rendering index of transmitted light through transparent part of combined PV-vacuum glazing for both 35% and 42% were calculated using Eqs.

Table 1
Solar, luminous and UV transmittance and reflectance of combined PV-Vacuum glazing, vacuum and single glazing.

	Combined PV-Vacuum glazing	Vacuum glazing	Single glazing
UV transmittance (280 nm-380 nm)	18%	20%	47%
Luminous transmittance (380 nm-780 nm)	64%	77%	94%
Solar transmittance (300 nm −2500 nm)	33%	43%	93%
UV reflectance	11%	16%	9%
Luminous reflectance	20%	14%	8%
Solar reflectance	40%	37%	7%

glazing than single glazing's behaviour. This combined glazing has 40% solar reflectance, which is close to vacuum glazing 37% reflectance. This reflectance was due to low emission coating which restricts to admit solar transmission.

4.2. Glazing factors

Solar factor or solar heat gain coefficient of combined PV-vacuum glazing was calculated using equation (7). For vertical plane glazing, external heat transfer coefficient was 25 W/m^{2}K and internal heat transfer coefficient was 7.7 W/m^{2}K. The external ambient temperature was 10 °C and wind speed was 4 m/s. The internal ambient temperature was 20 °C and wind speed of 0.3 m/s. Results of solar factors are listed in Table 2. Solar skin protection factor (SSPF) and solar material protection factor (SMPF) for this combined glazing were found to be 0.68 and 0.45 respectively. Under direct sunlight exposure, to achieve a high protection level, the SMPF and SSPF values for the window panes need to be increased.

Comparing with vacuum and single glazing, it is evident that the two glazing panes give better protection than single pane counterparts. Thus PV −vacuum glazing gave higher SSPF and SMPF than other two glazings. Relatively low SMPF and high SSPF values, also give an understanding that indoor house materials such as books

Table 2
Glazing factor for combined PV-vacuum, vacuum and single glazing.

	Combined PV-Vacuum	Vacuum glazing	Single glazing
SSPF	0.68	0.63	0.29
SMPF	0.45	0.36	0.15
SF	0.41 (35% transparent) 0.48 (42% transparent)	0.47	0.93

(10) and (14) respectively and shown in Fig. 6. Results were compared with single and vacuum glazing. Admitted daylight through 20% and 37% semi-transparent PV-vacuum glazing both had high CCT (6360K) and CRI (96.7). Due to no distortion of entering daylight, quality of indoor daylight match closely with external daylight. Aesthetics and occupants' health and working environment will be enhanced by this high quality indoor daylight through this combined PV glazing. This high CCT and CRI for this semi-transparent glazing were very similar to single and vacuum glazing. Interestingly overall transparency of single glazing was 94% and vacuum glazing was 77%, whereas this combined glazings had 35% and 42%. However, the light quality of PV vacuum glazing was similar to the other two glazings.

CCT and CRI for this semi-transparent (both 35% and 42%) PV-vacuum glazing was also compared with 30% and 40% transparent SPD glazing as shown in Fig. 7. For SPD glazing's 30% and 40% transparent state, CCTs were 4900 K and 5202 K respectively and CRIs were 87 and 91 respectively as listed in Table 3 [49]. However,

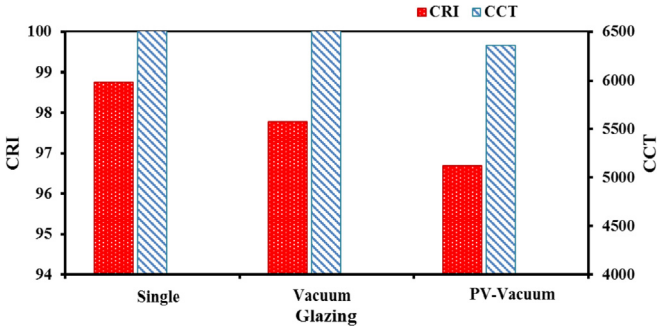

Fig. 6. CCT and CRI for PV vacuum, vacuum and single glazing.

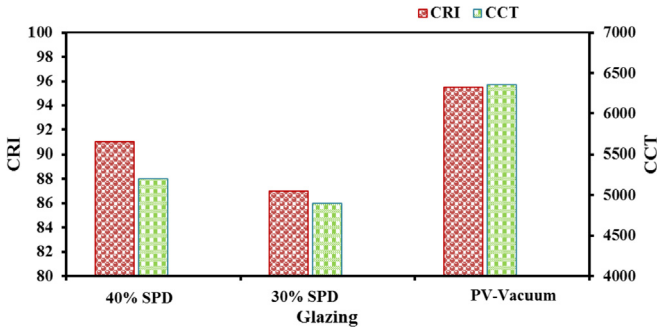

Fig. 7. CCT and CRI for 20% transparent SPD, and PV-Vacuum glazing.

SPD glazing offers suitable CCT and CRI for its transparent state. To achieve 30% and 40% transparent for SPD glazing or any other electrically activated switchable glazings (Electrochromic, Liquid Crystal) need power. This proposed semi-transparent PV-vacuum glazing offers power at this low transmission while light quality entering through the transparent part between PV cells are high and similar to natural daylight. Due to material behaviour and their own spectral variability, distortion of daylight occurs during admittance through SPD glazing into an indoor space. No distortion is present for PV-vacuum glazing as light passes through only glass. Thus, 35% and 42% both overall transmission showed an equal amount of CCT and CRI.

5. Conclusions

In this paper, first multicrystalline based combined PV-vacuum glazing has been introduced. This combined PV-vacuum glazing was semi-transparent in nature with 35% and 42% transparent depending on different PV area coverage. Mature, low cost, highly durable and high efficiencies are the advantages of multicrystalline-based PV. Thin film and third generation DSSC and perovskite type PV material transparency can be modulated by changing the material thickness. However these thin materials have low power conversion efficiency and unstable under ambient conditions.

Advantages of this type of semi-transparent PV-vacuum glazings are.

- No distortion of admitted daylight into indoor space as they penetrate through only glass;
- High CRI and CCT were found for 35% and 42% overall semi-transparent PV-vacuum glazing;
- This semi-transparent PV-vacuum glazing offered higher allowable CCT and CRI than 30% and 40% transparent states of SPD glazing;
- Lower SF compared to vacuum and single glazing
- Higher skin protection factor and material protection factors were found compared to solo single and vacuum glazing. Further improvement is possible using extra UV protective layer

This semi-transparent type glazing has potential to reduce overall transmission by covering glazing area with PV while quality of entering daylight is also maintained by keeping high CRI and CCT. To achieve semitransparency electrically activated switchable needs power whereas this PV-vacuum glazing generates power. Distortion of daylight is expected to be minimal for this type of semitransparency, as light will filter through glass rather than PV material. Thus, the colour rendering of indoor objects is minimal. This low heat loss combined PV–vacuum glazing has potential suitability in adaptive low energy building application due to its aesthetic advantages.

Acknowledgement

This work has been conducted as part of the research project 'Joint UK-India Clean Energy Centre (JUICE)' which is funded by the RCUK's Energy Programme (contract no: EP/P003605/1). The project's funders were not directly involved in the writing of this article. In support of open access research, all underlying article materials (data, models) can be accessed upon request via email to the corresponding author.

References

[1] A. Ghosh, B. Norton, Advances in switchable and highly insulating autonomous (self-powered) glazing systems for adaptive low energy buildings, Renew. Energy 126 (2018) 1003–1031, https://doi.org/10.1016/j.renene.2018.04.038.
[2] W.J. Hee, M.A. Alghoul, B. Bakhtyar, O. Elayeb, M.A. Shameri, M.S. Alrubaih, K. Sopian, The role of window glazing on daylighting and energy saving in buildings, Renew. Sustain. Energy Rev. 42 (2015) 323–343, https://doi.org/10.1016/j.rser.2014.09.020.
[3] H. Ye, X. Meng, L. Long, B. Xu, The route to a perfect window, Renew. Energy 55 (2013) 448–455, https://doi.org/10.1016/j.renene.2013.01.003.
[4] A. Ghosh, B. Norton, A. Duffy, Measured thermal & daylight performance of an evacuated glazing using an outdoor test cell, Appl. Energy 177 (2016) 196–203, https://doi.org/10.1016/j.apenergy.2016.05.118.
[5] Y. Fang, T.J. Hyde, F. Arya, N. Hewitt, P.C. Eames, B. Norton, S. Miller, Indium alloy-sealed vacuum glazing development and context, Renew. Sustain. Energy Rev. 37 (2014) 480–501, https://doi.org/10.1016/j.rser.2014.05.029.
[6] R.E. Collins, S.J. Robinson, Evacuated glazing, Sol. Energy 47 (1991) 27–38, https://doi.org/10.1016/0038-092X(91)90060-A.
[7] R.E. Collins, A.C. Fischer-Cripps, J.Z. Tang, Transparent evacuated insulation, Sol. Energy 49 (1992) 333–350, https://doi.org/10.1016/0038-092X(92)90106-K.
[8] P.W. Griffiths, M. Di Leo, P. Cartwright, P.C. Eames, P. Yianoulis, G. Leftheriotis, B. Norton, Fabrication of evacuated glazing at low temperature, Sol. Energy 63 (1998) 243–249, https://doi.org/10.1016/S0038-092X(98)00019-X.
[9] S. Memon, F. Farukh, P.C. Eames, V.V. Silberschmidt, A new low-temperature hermetic composite edge seal for the fabrication of triple vacuum glazing, Vacuum 120 (2015) 73–82, https://doi.org/10.1016/j.vacuum.2015.06.024.
[10] J. Zhao, S. Luo, X. Zhang, W. Xu, Preparation of a transparent supporting spacer array for vacuum glazing, Vacuum 93 (2013) 60–64, https://doi.org/10.1016/j.vacuum.2013.01.002.
[11] Y. Fang, P.C. Eames, B. Norton, T.J. Hyde, Experimental validation of a numerical model for heat transfer in vacuum glazing, Sol. Energy 80 (2006) 564–577, https://doi.org/10.1016/j.solener.2005.04.002.
[12] Y. Fang, T. Hyde, N. Hewitt, P.C. Eames, B. Norton, Comparison of vacuum glazing thermal performance predicted using two- and three-dimensional models and their experimental validation, Sol. Energy Mater. Sol. Cells 93 (2009) 1492–1498, https://doi.org/10.1016/j.solmat.2009.03.025.
[13] A. Ghosh, B. Norton, A. Duffy, Effect of sky clearness index on transmission of evacuated (vacuum) glazing, Renew. Energy 105 (2017) 160–166, https://doi.org/10.1016/j.renene.2016.12.056.
[14] C.G. Granqvist, I. Bayrak Pehlivan, G.A. Niklasson, Electrochromics on a roll: web-coating and lamination for smart windows, Surf. Coatings Technol. (2017) 6–11, https://doi.org/10.1016/j.surfcoat.2017.08.006.
[15] A. Ghosh, B. Norton, A. Duffy, First outdoor characterisation of a PV powered suspended particle device switchable glazing, Sol. Energy Mater. Sol. Cells 157 (2016) 1–9, https://doi.org/10.1016/j.solmat.2016.05.013.
[16] A. Ghosh, B. Norton, A. Duffy, Measured thermal performance of a combined suspended particle switchable device evacuated glazing, Appl. Energy 169 (2016) 469–480, https://doi.org/10.1016/j.apenergy.2016.02.031.
[17] A. Ghosh, B. Norton, A. Duffy, Measured overall heat transfer coefficient of a suspended particle device switchable glazing, Appl. Energy 159 (2015) 362–369, https://doi.org/10.1016/j.apenergy.2015.09.019.
[18] A. Ghosh, B. Norton, A. Duffy, Behaviour of a SPD switchable glazing in an outdoor test cell with heat removal under varying weather conditions, Appl. Energy 180 (2016) 695–706, https://doi.org/10.1016/j.apenergy.2016.08.029.
[19] A. Ghosh, B. Norton, Durability of switching behaviour after outdoor exposure for a suspended particle device switchable glazing, Sol. Energy Mater. Sol. Cells 163 (2017) 178–184, https://doi.org/10.1016/j.solmat.2017.01.036.
[20] A. Ghosh, B. Norton, A. Duffy, Daylighting performance and glare calculation of a suspended particle device switchable glazing, Sol. Energy 132 (2016) 114–128. https://doi.org/10.1016/j.solener.2016.02.051.
[21] A. Ghosh, B. Norton, T.K. Mallick, Solar Energy Materials and Solar Cells Daylight characteristics of a polymer dispersed liquid crystal switchable glazing, Sol. Energy Mater. Sol. Cells 174 (2018) 572–576, https://doi.org/10.1016/j.solmat.2017.09.047.

[22] D. Jung, W. Choi, J.-Y. Park, K.B. Kim, N. Lee, Y. Seo, H.S. Kim, N.K. Kong, Inorganic gel and liquid crystal based smart window using silica sol-gel process, Sol. Energy Mater. Sol. Cells 159 (2017) 488–495, https://doi.org/10.1016/j.solmat.2016.10.001.
[23] N. Skandalos, D. Karamanis, PV glazing technologies, Renew. Sustain. Energy Rev. 49 (2015) 306–322, https://doi.org/10.1016/j.rser.2015.04.145.
[24] A. Ghosh, B. Norton, A. Duffy, Effect of atmospheric transmittance on performance of adaptive SPD-vacuum switchable glazing, Sol. Energy Mater. Sol. Cells 161 (2017) 424–431, https://doi.org/10.1016/j.solmat.2016.12.022.
[25] Y. Fang, T. Hyde, N. Hewitt, P.C. Eames, B. Norton, Thermal performance analysis of an electrochromic vacuum glazing with low emittance coatings, Sol. Energy 84 (2010) 516–525, https://doi.org/10.1016/j.solener.2009.02.007.
[26] Y. Fang, P.C. Eames, Thermal performance of an electrochromic vacuum glazing, Energy Convers. Manag. 47 (2006) 3602–3610, https://doi.org/10.1016/j.enconman.2006.03.016.
[27] B. Norton, P.C. Eames, T.K. Mallick, M.J. Huang, S.J. McCormack, J.D. Mondol, Y.G. Yohanis, Enhancing the performance of building integrated photovoltaics, Sol. Energy 85 (2011) 1629–1664, https://doi.org/10.1016/j.solener.2009.10.004.
[28] A. Mutalikdesai, S.K. Ramasesha, Solution process for fabrication of thin film CdS/CdTe photovoltaic cell for building integration, Thin Solid Films 632 (2017) 73–78, https://doi.org/10.1016/j.tsf.2017.04.036.
[29] C.-H. Young, Y.-L. Chen, P.-C. Chen, Heat insulation solar glass and application on energy efficiency buildings, Energy Build. 78 (2014) 66–78, https://doi.org/10.1016/j.enbuild.2014.04.012.
[30] A. Ghosh, P. Selvaraj, S. Sundaram, T.K. Mallick, The colour rendering index and correlated colour temperature of dye-sensitized solar cell for adaptive glazing application, Sol. Energy 163 (2018) 537–544, https://doi.org/10.1016/j.solener.2018.02.021.
[31] J.W. Lee, J. Park, H.J. Jung, A feasibility study on a building's window system based on dye-sensitized solar cells, Energy Build. 81 (2014) 38–47, https://doi.org/10.1016/j.enbuild.2014.06.010.
[32] A. Cannavale, L. Ierardi, M. Hörantner, G.E. Eperon, H.J. Snaith, U. Ayr, F. Martellotta, Improving energy and visual performance in offices using building integrated perovskite-based solar cells: a case study in Southern Italy, Appl. Energy 205 (2017) 834–846, https://doi.org/10.1016/j.apenergy.2017.08.112.
[33] M.I. Asghar, J. Zhang, H. Wang, P.D. Lund, Device stability of perovskite solar cells – a review, Renew. Sustain. Energy Rev. 77 (2017) 131–146, https://doi.org/10.1016/j.rser.2017.04.003.
[34] S. Shalini, R. Balasundara Prabhu, S. Prasanna, T.K. Mallick, S. Senthilarasu, Review on natural dye sensitized solar cells: operation, materials and methods, Renew. Sustain. Energy Rev. 51 (2015) 1306–1325, https://doi.org/10.1016/j.rser.2015.07.052.
[35] A. Takeoka, S. Kouzuma, H. Tanaka, H. Inoue, K. Murata, M. Morizane, N. Nakamura, H. Nishiwaki, M. Ohnishi, S. Nakano, Y. Kuwano, Development and application of see-through a-Si solar cells, Sol. Energy Mater. Sol. Cells 29 (1993) 243–252, https://doi.org/10.1016/0927-0248(93)90039-6.
[36] A. Louwen, W. Van Sark, R. Schropp, A. Faaij, A cost roadmap for silicon heterojunction solar cells, Sol. Energy Mater. Sol. Cells 147 (2016) 295–314, https://doi.org/10.1016/j.solmat.2015.12.026.
[37] G. del Coso, C. del Cañizo, W.C. Sinke, The impact of silicon feedstock on the PV module cost, Sol. Energy Mater. Sol. Cells 94 (2010) 345–349, https://doi.org/10.1016/j.solmat.2009.10.011.
[38] J.M. Serra, J.M. Alves, A.M. Vallera, Progress and challenges for cost effective kerfless Silicon crystal growth for PV application, J. Cryst. Growth 468 (2017) 590–594, https://doi.org/10.1016/j.jcrysgro.2016.09.060.
[39] K.E. Park, G.H. Kang, H.I. Kim, G.J. Yu, J.T. Kim, Analysis of thermal and electrical performance of semi-transparent photovoltaic (PV) module, Energy 35 (2010) 2681–2687, https://doi.org/10.1016/j.energy.2009.07.019.
[40] T.Y.Y. Fung, H. Yang, Study on thermal performance of semi-transparent building-integrated photovoltaic glazings, Energy Build. 40 (2008) 341–350, https://doi.org/10.1016/j.enbuild.2007.03.002.
[41] W. Zhang, L. Lu, X. Chen, Performance evaluation of vacuum photovoltaic insulated glass unit, Energy Procedia 105 (2017) 322–326, https://doi.org/10.1016/j.egypro.2017.03.321.
[42] C. Chain, D. Dumortier, M. Fontoynont, A comprehensive model of luminance, correlated colour temperature and spectral distribution of skylight: comparison with experimental data, Sol. Energy 65 (1999) 285–295. https://doi.org/10.1016/S0038-092X(98)00145-5.
[43] C. Chain, D. Dumortier, M. Fontoynont, Consideration of daylight's colour, Energy Build. 33 (2001) 193–198, https://doi.org/10.1016/S0378-7788(00)00081-5.
[44] M.K. Gunde, U.O. Krašovec, W.J. Platzer, Color rendering properties of interior lighting influenced by a switchable window, J. Opt. Soc. Am. A 22 (2005) 416, https://doi.org/10.1364/JOSAA.22.000416.
[45] B.P. Jelle, A. Gustavsen, T.N. Nilsen, T. Jacobsen, Solar material protection factor (SMPF) and solar skin protection factor (SSPF) for window panes and other glass structures in buildings, Sol. Energy Mater. Sol. Cells 91 (2007) 342–354, https://doi.org/10.1016/j.solmat.2006.10.017.
[46] B.P. Jelle, Solar radiation glazing factors for window panes, glass structures and electrochromic windows in buildings - measurement and calculation, Sol. Energy Mater. Sol. Cells 116 (2013) 291–323, https://doi.org/10.1016/j.solmat.2013.04.032.
[47] F.J. Moralejo-Vázquez, N. Martín-Chivelet, L. Olivieri, E. Caamaño-Martín, Luminous and solar characterization of PV modules for building integration, Energy Build. 103 (2015) 326–337, https://doi.org/10.1016/j.enbuild.2015.06.067.
[48] C.S. McCamy, Correlated color temperature as an explicit function of chromaticity coordinates, Color Res. Appl. 17 (1992) 142–144, https://doi.org/10.1002/col.5080170211.
[49] A. Ghosh, B. Norton, Interior colour rendering of daylight transmitted through a suspended particle device switchable glazing, Sol. Energy Mater. Sol. Cells 163 (2017) 218–223, https://doi.org/10.1016/j.solmat.2017.01.041.